Study of the Impact of Visual and Haptic Sensory Sensitivities on the Detection of Visuo-Haptic Illusions in Virtual Reality

Flavien Lebrun, Sinan Haliyo, Malika Auvray, David Gueorguiev, Gilles Bailly

Study of the Impact of Visual and Haptic Sensory Sensitivities on the Detection of Visuo-Haptic Illusions in Virtual Reality
Étude de l'impact des sensibilités sensorielles visuelles et haptiques sur la détection d'illusions visuo-haptiques en réalité virtuelle

FLAVIEN LEBRUN, Université d'Evry Paris Saclay, IBISC, France
SINAN HALIYO, Sorbonne University, CNRS, ISIR, France
MALIKA AUVRAY, Sorbonne University, CNRS, ISIR, France
DAVID GUEORGUIEV, Sorbonne University, CNRS, ISIR, France
GILLES BAILLY, Sorbonne University, CNRS, ISIR, France

Visuo-haptic illusions enhance the user experience in virtual reality when physical resources are limited. In order to tailor these illusions to individual user characteristics, we argue in this paper that quantifying users' visual and proprioceptive sensitivities is essential. We thus present a method - comprising an experimental protocol and Bayesian analysis - for capturing human visual and proprioceptive sensitivity in virtual reality. Our findings demonstrate that 1) in accordance with existing literature, the visual modality is more precise in the azimuthal direction, and proprioceptive precision is higher in depth; 2) the visual and proprioceptive precisions achieved in VR are of a similar magnitude, in contrast to real-world literature results; 3) it is possible to categorize participants based on their proprioceptive and visual precisions. These results will serve as a foundation for studying the impact of human sensitivities on the perception of visuo-haptic illusions.

Les illusions visuo-haptiques permettent d'enrichir l'expérience utilisateur en réalité virtuelle lorsque les ressources physiques sont limitées. Afin d'adapter ces illusions aux caractéristiques individuelles des utilisateurs nous argumentons dans cet article que la quantification des sensibilités visuelle et proprioceptive des utilisateurs est essentiel. Nous présentons donc une méthode – protocole expérimental et analyse bayésienne – pour capturer la sensibilité visuelle et proprioceptive humaine en réalité virtuelle. Nos résultats montrent que 1) conformément à la littérature, la modalité visuelle est plus précise dans la direction azimutal et la précision proprioceptive est plus précise en profondeur ; 2) les précisions visuelles et proprioceptives obtenues en RV sont de même ordre de grandeur contrairement aux résultats de la littérature en environnement réel ; 3) il est possible de classer les participants selon leurs précisions proprioceptive et visuelle. Ces résultats serviront de base pour étudier l'influence des sensibilités humain sur la perception des illusions visuo-haptiques.

CCS Concepts: • **Human-centered computing → HCI theory, concepts and models**; *Pointing*; Visualization techniques.

Additional Key Words and Phrases: Interaction technique, Models

Mots Clés et Phrases Supplémentaires: Techniques d'interaction, Modèles

Reference:
Flavien Lebrun, Sinan Haliyo, Malika Auvray, David Gueorguiev, and Gilles Bailly. 2024. Study of the Impact of Visual and Haptic Sensory Sensitivities on the Detection of Visuo-Haptic Illusions in Virtual Reality.

1 INTRODUCTION

Visuo-haptic illusions rely on a mismatch between the visual and haptic information coming from the same physical event. To solve this mismatch, the brain often favors perception coming from the visual modality [7, 46]. Thus, the visual information can "manipulate" the multi-modal perception of physical events and compensate for the lack of

2024.

realism of the haptic information. Visuo-haptic illusions are used in virtual reality (VR) to reduce the limitations of mechanical haptic interfaces by expanding their perceived workspace or resolution [1, 22]. They allow redirecting a user's movements towards selected real objects, enabling a real object to serve as physical counterpart for several virtual objects [3]. They also provide physicality to virtual objects without or with limited haptic stimulations [38, 63].

A key parameter of visuo-haptic illusion is the amplitude, which corresponds to the gap between the visual and haptic information. When this amplitude is too important for the brain to solve the sensory mismatch, the users "detect" the illusion , which leads to a decrease in presence in VR. In practice, VR designers need to know when users are likely to detect illusions to maintain a high level of immersion. Importantly, the ability to detect illusions vary among individuals [37]. Our long term goal is to develop adaptive visuo-haptic illusion techniques, i.e., techniques that adapt the illusion to the perceptual abilities of each individual. Such adaptive techniques raise to challenges : (1) estimating the perceptual abilities of each individual and (2) elaborating a computational model.

In this article, we address the first challenge: *how to measure the sensitivity of a given modality in virtual reality ?* More precisely, we aim to address the three following research sub-questions:

- RQ1: Is there an appropriate methodology to measure visual and proprioceptive sensitivities?
- RQ2: How do the sensory sensitivities of participants in Virtual Reality compare to the ones in the real world?
- RQ3: Is it possible to differentiate users based on their visual and proprioceptive sensitivities?

To address these research sub-questions we rely on experimental protocols and analysis methods derived from cognitive psychology [59]. These studies were conducted in a real environment, and we hypothesize that the precision of certain modalities may differ in VR (RQ2).

We firs provide a brief overview of visuo-haptic illusion techniques and discuss how they correlate with the precision of the user's sensory modalities. We then introduce a methodology to experimentally estimate these precisions for both a population and an individual. This methodology is applied in an evaluation campaign, which is analyzed using a conventional approach from the literature, as well as a Bayesian analysis technique. This analysis demonstrates, on one hand, that the precisions of certain modalities differ between VR and real environments. It also shows that Bayesian analysis allows for the calculation of individual parameters, which can be leveraged for personalizing an illusion.

2 RELATED WORK

In this section, we describe visuo-haptic illusions in VR and their applications.

2.1 Visuo-Haptic Illusions in Virtual Reality

Several interaction techniques based on visual illusions have been proposed in virtual reality. The common feature among these illusions is the manipulation of the visual rendering of the virtual environment. Although some of these illusions are based on a shift between visual and vestibular [48] or auditory information [50], we primarily focus on visuo-haptic illusions [1]. Indeed, this family of illusions enhances haptic interactions in VR. Almost all these illusions involve the manipulation of the visual rendering of the virtual hand of the user or of a tool manipulated by the user.

The manipulation of the visual rendering can involve the color or shape of objects or the user's avatar's skin to influence tactile perceptions of object characteristics, such as their stiffness [2, 4, 47]. However most of visuo-haptic illusions deceive proprioception by introducing a difference between the movements of the real body and those of the

[1]These illusions are often collectively referred to as "pseudo-haptic" [38, 63], although a family of illusions called "redirection" [3, 35] is often dissociated from this classification.

corresponding virtual avatar. This can alter the perception of an object's weight [13, 28, 53], the number of physical objects in the scene [3, 8, 34], or the stiffness of a spring [39]. For instance, the technique of "Hand Redirection" [3, 8, 33] introduces a gradual offset between a user's real hand and their virtual avatar during a movement. This offset is continuously corrected, resulting in a change in the real hand's trajectory. In extreme cases, the user's hand can be redirected toward a single physical object when moving towards different virtual objects [3, 8, 34]. In this article we focus on the study of visuo-haptic illusion that involve a shift between the real hand (proprioceptive perception) and the virtual hand (visual perception).

2.2 Detection of Illusion

The brain rejects an illusion if it notices that something is wrong. Several studies aimed to estimate the maximum amplitude beyond which participants (*population level*) notice it or judge it uncomfortable [1, 7, 8, 21, 23, 30, 44, 51, 69] However, these detection thresholds are low and can be increased by customizing the implementation of illusions to each participant's characteristics (*individual level*). Lebrun et al. [37] show that it is possible, after a short calibration phase, to adjust the amplitude of hand redirection for each participant and thus increase the detection threshold in comparison with the one obtained at the population level. Groth et al. [24] also find that there exists a difference in gender for the detection of hand redirection illusions. They demonstrate that for a similar amplitude the detection probabilities of women are significantly lower. Yet, to our knowledge, no study has attempted to explain the differences between participants using computational models. We justify the importance of users sensitivities for the implementation of such models in the following section.

3 HYPOTHESIS AND THEORETICAL FOUNDATION

We make the hypothesis that the ability of the users to estimate the positions of the physical and virtual hand has an impact on the likelihood of detecting the Hand Redirection illusion. We describe here two mechanisms that can lead to the detection of illusion. The first is linked to a decrease in users' sense of agency i.e a decrease in the experience of controlling one's own actions and, through them, changes in the external environment[25]. The second is linked to a decrease in the sense of body ownership (SoO). Body Ownership refers to one's self-attribution of a body [20, 61]. In this section, we demonstrate the importance of estimating individual sensitivities – particularly visual and proprioceptive – to predict the break of SoA and SoO and thus predict the detection of an illusion. To achieve this, we describe some computational models linked to the decrease in SoA and SoO.

3.0.1 Models about the Sense of Agency. The SoA is a component of the sense of presence [31]. A decrease of SoA can lead to users noticing that something is off. The comparator model [18] can explain a decrease of SoA (see 10 for a detailed explanation of the comparator model). According to this model, the brain creates an efferent copy whenever a new motor command is generated. If the efferent copy matches the actual sensory perception, the movement is perceived as self-caused, and SoA arises [10]. On the opposite, if the sensory perception and the efferent copy are too different, it could lead to a semantic break [45] and a decrease in SoA. Thus, the actual sensory perception plays an important role. In our context, the brain perception of the hand comes from an integration of discrepant information from the visual and proprioceptive modalities. To evaluate the value of this perceived position, one needs to understand how these two information are weighted to come up with a unified perception.

Computational models related to the optimal multi-sensory integration can help us predict the estimation of the hand position from the integration of visual and proprioceptive information. For instance, according to the Gaussian

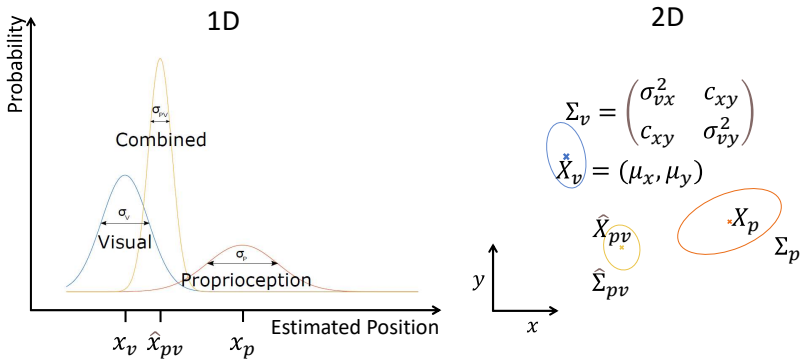

Fig. 1. Illustration of the model of optimal multi-sensory integration. On the left, the brain combines the visual information (x_v) and the proprioceptive information (x_p) in an optimal manner. The estimated position $\hat{x_{pv}}$ is closer to x_v than x_p because the confidence in the visual information (small variance σ_v) is better than the proprioceptive one (large variance σ_p). The variance σ_{pv} is smaller than either σ_v or σ_p. On the right we illustrate a similar optimal integration for 2D positioning instead of 1D. Here the confidence in a positional information is represented by confidence ellipse. These ellipses have 3 parameters, the x and y variance and the covariance, that describe the relative elongation and orientation of the ellipse.

association model [15], the estimation of a quantity by a combination of different modalities (e.g. vision+proprioception) depends on the confidence that the brain has in each modality. This confidence is characterized by the sensitivity of the corresponding modality. Consider the estimation of the x position of an object (1D estimation) by the visual and proprioceptive modalities (Figure 1-Left). The sensitivity of these modalities can be mathematically represented by their corresponding variances: σ_v^2 for the **v**ision and σ_p^2 for the **p**roprioception. The final position estimation of the object by the brain $\hat{x_{pv}}$ is thus a weighted combination of the estimation made by the visual x_v and proprioceptive x_p modalities:

$$\hat{x_{pv}} = \frac{\sigma_p^2}{\sigma_v^2 + \sigma_p^2} x_v + \frac{\sigma_v^2}{\sigma_v^2 + \sigma_p^2} x_p \tag{1}$$

The final estimation x_{pv} is more precise than the most precise modality estimation (see Figure 1). Moreover, the less precise the estimation of a modality is (i.e. large variance), the less influence it has on the final estimation of the quantity. The integration is "optimal" in that sense that it minimizes the error of the estimation of the physical quantity.

The brain seems to follow this integration pattern for physical quantities such as the size of an object through vision and haptics [14], the orientation of the body in space through vision and the vestibular system [16, 70], the shape of an object by vision and touch [26] and the localization of our limbs during a movement [6, 57, 58, 65–67].

3.0.2 Models about the Sense of Ownership. The SoO is also a component of the sense of presence. Like the SoA, a decrease in SoO can lead to the detection of an illusion. Bayesian Causal inference models [36] explain the sense of ownership (SoO) in VR [32]. These models propose that the SoO emerges as the result of attributing all sensory information available about the body to a single common cause: the self-body [52, 54]. In our case the brain decides to attribute the visual (x_v) and proprioceptive (x_p) position of the hand to a common cause (C=1) or to a different cause (C=2). If the virtual hand is seen as the cause of both x_v and x_p (C=1) there is a SoO toward the virtual hand, else if the virtual hand is only the cause of x_v (C=2), no SoO occurs (see Figure 2).

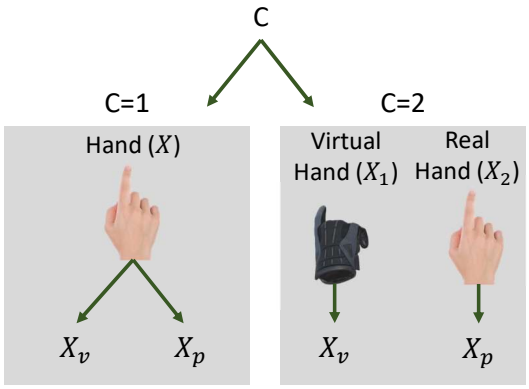

Fig. 2. Illustration of the causal inference. Left (C=1), the brain infers that visual and proprioceptive information have the same cause: the hand. The virtual hand is considered to be also the source of the proprioceptive information (coming from the real hand), this results in a SoO toward the virtual hand. The two positional estimation x_v and x_p are integrated to one unified estimation of the hand position x. Right (C=2) the brain infers that visual information (virtual hand) and proprioceptive information (read hand) comes from independent causes: The brain perceives two different positions x_1 and x_2 and then dissociates the virtual and the real hands.

To select the most likely cause the brain infers each cause probability considering the available information: $P(C1|X_v, X_p)$ and $P(C2|X_v, X_p)$. The Bayes's theorem is used to calculate these probabilities:

$$P(C = i|x_v, x_p) = \frac{P(x_v, x_p|C = i) \times P(C = i)}{P(x_v, x_p)} \tag{2}$$

where i equals 1 or 2. In this equation, $P(C = 1)$ is the prior probability of a common cause and $P(C = 2)$ the prior probability of a different cause. These two prior probabilities are fixed by the brain and do not depend on the sensory sensitivity. The term $P(x_v, x_p)$ is constant and can be disregarded when comparing $P(C = 1|x_v, x_p)$ and $P(C = 2|x_v, x_p)$. Finally $P(x_v, x_p|C = 1)$ and $P(x_v, x_p|C = 2)$ are the likelihoods of having the positions of the hand at x_v and x_p given C=1 or C=2. These likelihoods are calculated based on users' visual and proprioceptive sensory sensitivities.

Therefore to predict both the breaks in SoA and SoO with computational models, it is necessary to first capture and measure users' visual and proprioceptive sensory sensitivities.

4 MEASURES OF SENSORY SENSITIVITIES

Problem formulation. The task we consider in this work is a pointing task in VR with the right hand. The specificities of this task are that 1) two modalities are involved (vision and proprioception) and 2) a pointing movement involves multiple joints (wrist, elbow, shoulder and potentially finger) and 3) we consider two quantities (the final x an y positions). Our objective is to estimate the visual sensitivity S_V of the users as well as the proprioceptive sensitivity of their right hand $S_{P_{RH}}$ for this task. While it is easy to estimate an overall sensitivity GS_1 by measuring, for instance, the dispersion of the final hand points, it is difficult to estimate the respective contribution of each modality. From a mathematical point of view, the problem consists of resolving a single equation with two unknowns:

$$GS1 = f(S_V, S_{P_{RH}}) \tag{3}$$

Both sensitivities S_V and $S_{P_{RH}}$ can be decomposed into precision *i.e. the variance of the distribution*, and accuracy *i.e. the systematic bias*.

Common experimental protocols. 2 main experimental protocols have been proposed in the literature to measure the sensory sensitivity of modalities.

One protocol consists of simply asking participants to perform several times the same pointing task (estimating quantities). With several repetitions, the participants form a distribution whose variance and mean can be extracted. The mean inform on the accuracy and the variance on the precision. The global sensitivity of this task is thus the measure of this variance and mean. A variant of this protocol has been extensively used in health and sports to measure proprioceptive sensitivity for multiple joints (e.g. the ankle [12] or the knee [62]). It was possible because the task did not involve vision. In our context, the global proprioceptive sensitivity of the right hand $S_{P_{RH}}$ also depends on the proprioceptive sensitivity of multiple involved joints. While it could be informative to measure the sensitivity of each joint, this approach is time-consuming, tedius and not necessary to study visuo-haptic illusion.

Another protocol [14, 41] is based on a 2AFC experiment. The participants compare two quantities (e.g., the size of an object [14]) and should estimate which one of the two quantities is smaller/larger (forced choice). The more finely a participant can discriminate the two quantities with one modality, the greater the accuracy of this modality is. This 2AFC protocol has been used in different contexts [49], [42], [27].

Limitations. These two protocols do not allow to distinguish the visual and proprioceptive sensitivities of each modality for a pointing task. One can consider suppressing one modality when performing the pointing task to measure the sensitivity of the other modality. However, it is extremely challenging. For instance, if the visual modality is suppressed, the stimulus, the target, is not visible. It would require to carry the hand of the participant to defined positions. Beyond the difficulty (time and setup) to implement such study, it remains that the participants would perform passive movements instead of active movements. Similarly, it would also be possible to suppress the proprioceptive modality, but it would require invasive operations (anesthesia). To solve this problem, Van Beers et al. [64] proposed an original method on which we build on to measure users' sensitivities.

Van Beers et al. protocol. The Van Beers et al. protocol [64] aims to assess the precision of human hand proprioceptive localization. Their findings indicate that for proprioception, localization in the radial direction relative to the shoulder exhibits greater precision compared to localization in the azimuthal direction. Regarding visual localization, their observations reveal that localization in the azimuthal direction relative to the cyclopean eye demonstrates higher precision than localization in the radial direction. In their protocol the participants perform three different (pointing) tasks (instead of one). From each task, a general sensitivity is extracted providing from a unique combination of visual sensitivity S_V, proprioception sensitivity of the right hand $S_{P_{RH}}$ and proprioception sensitivity of the left hand $S_{P_{LH}}$ (see Figure 3). More precisely:

(1) General sensitivity task 1 GS_1 is the combination of visual sensitivity S_v and the proprioceptive sensitivity of the right hand $S_{P_{RH}}$: $GS1 = f(S_V, S_{P_{RH}})$
(2) General sensitivity task 2 GS_2 is the combination of visual sensitivity S_v and the proprioceptive sensitivity of the left hand $S_{P_{LH}}$: $GS2 = g(S_V, S_{P_{LH}})$
(3) General sensitivity task 3 GS_3 is the combination of the proprioceptive sensitivity of the right hand $S_{P_{RH}}$ and the proprioceptive sensitivity of the left hand $S_{P_{LH}}$: $GS3 = h(S_{P_{RH}}, S_{P_{LH}})$

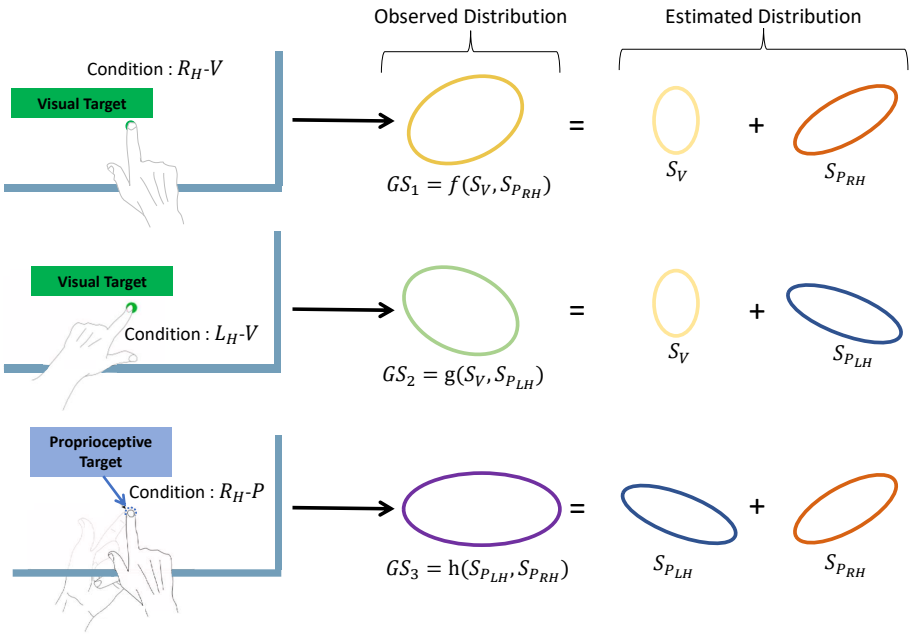

Fig. 3. Diagram illustrating the three different pointing tasks, each corresponding to an experimental condition. In the condition $R_H - V$ and $L_H - V$ the target is visual. In the condition $R_H - P$ the target is proprioceptive (the left hand under the table). With each condition pointing to the target several times will create a distribution of points. From this distribution (here represented directly to the right of the condition diagrams) we can extract the sensitivity of the modality that evaluates the target position and of the modality that evaluate the hand position. We obtain a system of three equations with three unknowns that can be solved.

In other words, one equation with two unknowns (which does not have a unique solution) is transformed into a system of three equations with three unknowns which has the advantage to have a unique solution.

Our general approach relies on this protocol. We now detail how we collected data in our context.

5 DATA COLLECTION

5.1 Participants and Apparatus

Twelve participants take part in the study. Their ages range from 25 to 32 years. There are 10 right-handed individuals and 2 left-handed individuals. Four participants wear glasses or contact lenses. None of the participants have any neuro-muscular disorders affecting their proprioception. All participants signe an informed consent form, and the study, in compliance with the Helsinki Declaration, is approved by the ethics committee of Sorbonne University (N° 2020 – CER- 2020- 61).

They wear an HTC Vive head mounted display tracked by an Optitrack system composed of 8 infrared cameras. The position and 3D orientation of the participants' index finger is also recorded with the Optitrack system, using a glove with markers.

Participants are sitting in front of a transparent Plexiglas table. 7 haptic targets are placed under the table. The locations of these targets are the same than the virtual targets that the participants can see in the HMD (see Figure 4).

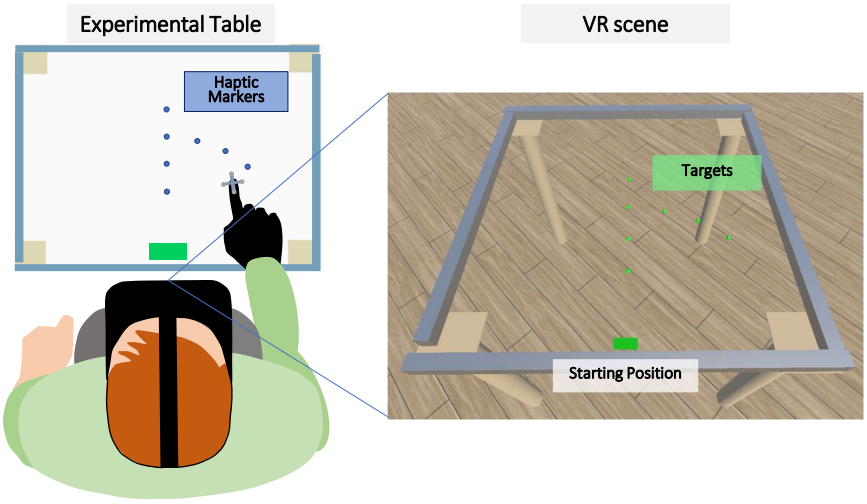

Fig. 4. On the left : illustration of the experimental setup in the real world. The participant is seated in front of transparent table wearing the HMD and a gloves with optitrack marker (on the left or right hand in fonction of the condition). Under the table 7 haptic markers are placed in the same position as the visual target displayed in VR. On the right : view of the participant in the VE. The position of the hand is never displayed in VR. The seven target (green) are all displayed here. However during the experiment participants will see only one at a time.

An additional haptic target indicates the starting position which is both felt and seen in VR. A pedal under the right foot of the participants is used to validate each trial. In the virtual environment, the participants do not see their hands.

5.2 Task and Conditions

The task consists of positioning the tip of their index finger as accurately as possible on one of the seven possible targets. Depending on the conditions, participants use either their right or left hand, virtual or physical targets.

- In the first condition, participants have to match as best as possible the position of the tip of the index finger of their **right hand** with the position of a visible **visual** target in the virtual environment : Right Hand - Visual Target $R_H - V$. The visual target is represented with a green sphere of the size of a thumb (see Figure 4)
- In the second condition, participants have to match the position of the tip of the index finger of their **left hand** with the position of a **visual** target in the virtual environment (Left Hand - Visual Target $L_H - V$)
- In the last condition, the participants have to match as well as possible the position of the tip of the index finger of their **right hand** on the table with the position of the index finger of their left hand placed under the table (Right Hand - Proprioceptive Target $R_H - P$). The left hand is positioned on a **physical** target. The physical targets have the same position and relative size as the visual targets, except that the thickness of the table separates them (~5mm).

Each participant performed the 3 conditions corresponding to the three tasks of the method (see Figure 3):

5.3 Procedure

We first explain the principle of the experiment to the participants and have them read and fill out a consent form. Then, they put on the HMD and glove, on their right hand for the $R_H - V$ and $R_H - P$ conditions and on their left hand for the $L_H - V$ condition. They then place their right foot on the pedal for all conditions. When they enter the VE, participants see a screen showing them their next task. They must press the foot pedal to begin the training phase. This phase is performed for each new condition.

In all conditions the participants, once the target has appeared, must place the hand wearing the glove (invisible in the VE) as best as possible on the position of this target. Once they are satisfied with the position of their hand, they must press the pedal. They must then return to the starting position to begin the next trial.

For the $R_H - V$ and $L_H - V$ conditions, the target is visual and appears as soon as the participants have reached the starting position. For the $R_H - P$ condition, the target is proprioceptive, it is the fingertip of the left hand. When participants start a new cycle (of $R_H - P$), a visual target appears. They must then place their left hand, under the table, on the haptic target corresponding to this position. They must then press the foot pedal. This causes the visual target to disappear and numerous visual targets to appear for 2 seconds. They act as a lure to make the participant forget the position of the visual target. The participant thus focuses only on the position of his left hand for the aiming task.

For the $R_H - V$ and $L_H - V$ conditions, participants perform 6 training cycles. For the $L_H - V$ condition, they perform 12 training cycles. Once the training phase is completed, the real experiment begins as soon as the participant is ready and presses the pedal. Participants aim 20 times at each of the 7 targets in the same way as they did in the training phase. The number of attempts already made is displayed on the virtual screen in front of them.

5.4 Design

This study follows a within-subjects design. The presentation order of the three conditions is counter-balanced between participants to avoid learning effects. For each condition, participants perform 20 blocks. In each block (7 trials), each target is presented one time in a random order. In summary the experimental design is: 12 participants x 3 conditions x 20 blocks x 7 targets = 5040 trials.

5.5 Measures

The 3 dependent variables are Precision and Accuracy of the index finger position as well as Time to reach the target.

5.6 Differences with Van Beers et Al. Protocol?

In Van Beers et al. [64] experiment, participants were situated in a real-world setting and seated facing a table. They observed the reflection of visual targets affixed to a cardboard above the tabletop using a horizontally mounted mirror placed midway between the cardboard and the table. This setup created the illusion for the subjects that the targets were positioned on the table. Notably, they employed only three targets, a reduced number compared to our seven targets. These targets were positioned relatively close to the body: one approximately 30cm from the body, slightly on the left, and another approximately 20cm from the body, slightly on the right. The spatial coverage of these targets concerning the user closely resembled that of our targets. Consequently, we contend that, at least as an approximate comparison, it is viable to juxtapose the averages derived from our obtained values with those obtained in their study.

6 ANALYSIS

6.1 Mathematical Formalization of Sensory sensitivity

We assume that the sensory sensitivity can be represented by a confidence ellipse which contains the final positions of the index finger (see Figure 1). We work in this study with 95% confidence ellipses. The distribution of points to form this ellipse can be generated by a 2-D Gaussian function. A 2D Gaussian is defined by its mean $\mu = (\mu_x,\mu_y)$ representing the center of the ellipse and by its covariance matrix Σ (see Figure 1) representing its shape:

$$\Sigma = \begin{pmatrix} \sigma_x^2 & c_{xy} \\ c_{xy} & \sigma_y^2 \end{pmatrix} \tag{4}$$

The covariance matrix has three parameters. The variances σ_x^2 and σ_y^2 characterize the elongation of the ellipse in a certain direction. The covariance c_{xy} gives the orientation of the ellipse. For example in Figure 1 the ellipse illustrating the proprioceptive sensitivity (orange) is more elongated in the x direction and therefore has a higher σ_x^2 than σ_y^2. It is the opposite for the ellipse representing the visual sensitivity (blue). None of these ellipses are oriented perfectly horizontally, therefore their covariance is different from 0.

The covariance matrix Σ represents the precision of the modality. Its accuracy corresponds to the offset between the target position and the center of the ellipse: $bi = (bi_x,bi_y)$. Note that in sensory integration models, the precision (i.e. covariance matrix Σ) is used to assign a weight to a modality.

6.2 Bimodal Data Analysis

The first step of the analysis is to put the observed data into an usable form. We have the final positions (p_x,p_y) of the left and right hand indexes (*FPI*). We have 21 (7 targets * 3 conditions) distributions for each participant. For each distribution, we calculate the 5 parameters (μ_x,μ_y,σ_x^2, σ_y^2,c_{xy}) of the 95% confidence ellipse. However, these *bimodal* confidence ellipses correspond to the combination of two sensitivities. We then need to extract each *unimodal* sensitivity individually. We propose two methods of analysis.

6.2.1 Classical Analysis. The classical method of analysis is the one used by Van Beers et al. [64]. For each condition, the two distributions, expressing the precision of the two modalities involved, are independent. Indeed the two modalities are measuring different physical elements. Thus the bimodal covariance matrix obtained is simply the sum of the two unimodal covariance matrices. Similarly the bias (bi) of the mean of the bimodal distribution is the sum of the biases of the unimodal distributions. For the condition $R_H - V$ for example this is expressed as follows:

$$\Sigma_{R_H-V} = \Sigma_V + \Sigma_{P_{R_H}} \tag{5}$$

$$bi_{R_H-V} = bi_V + bi_{P_{R_H}} \tag{6}$$

where Σ_{R_H-V} and bi_{R_H-V} are the covariance matrix and bias parameters of the observed bimodal distributions with the experiment, and bi_V, $bi_{P_{R_H}}$, Σ_V, $\Sigma_{P_{R_H}}$, and bi_{PM_D} are the bias and covariance matrix of the unimodal distributions representing the sensitivities of the visual (S_V) and of the right hand proprioceptive ($S_{P_{RH}}$) modalities. We can transpose the Equation 5 and the Equation 6.2.1 to the conditions $L_H - V$ and $R_H - P$. For each target, the 3 distributions obtained from the 3 conditions give a system of 3 equations with 3 unknowns (the unknowns being the 3 couples (bi_V, Σ_V), ($bi_{P_{R_H}}$, $\Sigma_{P_{R_H}}$), ($bi_{P_{L_H}}$, $\Sigma_{P_{L_H}}$). The Figure 3 illustrates the system of three equations with three unknowns. The resolution of this system provides the 3 couples of parameters describing each unimodal distribution. In summary:

- **Input (for each participant)**:
  - 21 bimodal distributions (bi, Σ) from 7 targets and 3 conditions
- **Algorithm for each target**:
  - Selection of the 3 bimodal distributions for each target (1 per condition)
  - Construction of the equation system with the 3 bimodal distributions
  - Solving the equation system
- **Output**:
  - 7 unimodal distributions (bi, Σ) for each of the 3 modalities (visual, right and left hand proprioception)

This method directly relies on our observations and has the advantage of proposing an exact solution. However, the resolution of the equation system imposes the use of subtractions for the calculation of unimodal distributions. This can lead to parameters with impossible values (due to measurement noise) such as negative variances. This problem is corrected if the results are averaged over all participants. Indeed there are more positives than negatives result which when averaged give a positive result. This method therefore provides a tool for studying modality sensitivities at the *population* level, but is not appropriate at the *individual* level.

6.2.2 Bayesian Analysis. To study our results at the individual level, we propose to turn the problem around. Instead of starting from the bimodal distribution and try to extract the unimodal distributions, we search the optimal unimodal parameters that will generate the observed (FPI) bimodal distribution. Indeed, with a Bayesian inference approach [5], the objective is not to find the exact value of one parameter (here the covariance matrix Σ) but rather a posterior probability law on this parameter Σ. That is to say the probability distribution of the parameter value after taking into account the experimental data. A Bayesian inference approach requires a prior law of the parameters that we want to estimate. The prior law reflects the knowledge about the value of the parameter before observing the data.

To implement the Bayesian inference approach, we use the ABC (Approximate Bayesian Computation) algorithm already used in the HCI community by [29]. The principle of ABC is to repeatedly generate a set of unimodal parameter values drawn from prior law. We can then calculate the bimodal gaussian law parameters and generate the bimodal points distribution. Finally, we compare the simulated distribution to the observed distribution (FPI). If the distance between the two distributions is close enough, the parameter values are accepted. We repeat this process n times. For each parameter, the accumulation of their accepted values define the parameters' probability law.

We have chosen to calculate the biases by the classical method presented in subsubsection 6.2.1 to limit the number of parameters. In summary :

- **Input for each participant:**
  - 21 bimodal distributions (bi, Σ) from 7 targets and 3 conditions
  - 3 prior laws of Σ parameters, one per modality
  - The values of the unimodal biases (bi) calculated with the classical method
- **Algorithm for each target:**
  WHILE n < 10000:
  - step 1: drawing of parameters Σ_V, Σ_{PM_D} and Σ_{PM_L} based on the chosen prior law (in total there are 3*3 = 9 parameters).
  - step 2: generation of the bimodal distributions (bi_{R_H-V}, Σ_{R_H-V}), (bi_{L_H-V}, Σ_{L_H-V}) and (bi_{R_H-P}, Σ_{R_H-P}) (see Equation 5 and Equation 6.2.1)

– step 3: creation of three PFI_{sim} datasets generated following the 3 2D Gaussian laws (bi_{M_D-V}, Σ_{M_D-V}), (bi_{M_G-V}, Σ_{M_G-V}) and (bi_{R_H-P}, Σ_{R_H-P})
– step 4: evaluation of the distance $d(PFI_{obs}, PFI_{sim})$ for the 3 conditions $R_H - V$, $L_H - V$ and $R_H - P$
– step 5: IF $d(PFI_{obs}, PFI) < \epsilon$ the parameters are accepted. ELSE the parameters are deleted
END WHILE
- final step: Draw the 9 parameters' probability laws from the accumulation of accepted parameter values

- **Output:**
- 9 probability laws on the covariance matrices Σ for the 3 modalities (visual, proprioceptive right hand and proprioceptive left hand).

The average of these probability laws is used to compare this method with the previous classical method, which provides unique values. To apply the ABC algorithm we used the software package *ELFI* [40]. We use a variation of the classical ABC algorithm called Sequential Monte Carlo ABC and compare the euclidean distance between the variance and the mean of the real and simulated distribution. This implementation was made under python.

6.3 Frame of Reference

The two variances σ_x^2 and σ_y^2 are expressed with respect to x and y coordinates. However, it is more interesting to express them in the frame of reference of the participant: depth and azimuth. Each covariance matrix obtained is thus now expressed along these axes.

7 RESULTS

7.1 Bimodal Data

The Figure 5 illustrates the distribution (PFI) averaged over all participants for the three conditions.

7.1.1 Precision. We observe that the confidence ellipses of the $R_H - V$ (right hand visual target; green) and $L_H - V$(left hand visual target; orange) conditions are close to a circle and slightly more elongated in the depth direction. In contrast, the confidence ellipses of the $R_H - P$ condition (right hand proprioceptive target; purple) are more elongated in the azimuthal direction.

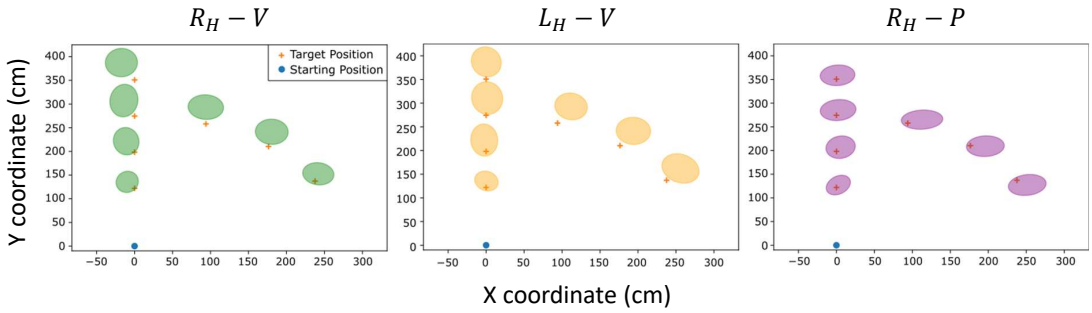

Fig. 5. Precision and accuracy for the seven targets and the three conditions. Left: Pointing with the right hand; Center: Pointing with the left hand; Right: Proprioceptive pointing with the right hand.

The Figure 6 compares precision in virtual reality (our data) with the precision in a real environment (data from [64]). The results suggest that the precision in virtual reality are aligned with those in a real environment (see section 5.6)[56, 64] : proprioception is more precise with respect to depth (Figure 6-left) and vision is more precise with respect to azimuthal direction (Figure 6-center).

The Figure 6-right also suggests that users are more precise in a real environment than a virtual one. We observed indeed on Figure 6-left a large depth variance of the conditions involving vision ($R_H - V$ and $L_H - V$) which is not compensated for by the small azimuthal variances (Figure 6-center).

7.1.2 Accuracy. We observe that participants tend to overreach targets in depth especially for the conditions involving vision. There is also a lateral overreach: for the condition visual pointing with the right hand ($R_H - V$), the pointing is shifted to the left, while for the condition pointing with the left hand ($L_H - V$), it is shifted to the right. Finally, for the condition with proprioceptive target ($R_H - P$), we observe a rightward overshoot.

The data on accuracy were analyzed only qualitatively in the original article [64]. Therefore, we cannot make quantitative comparisons. Qualitatively, our results on accuracy in virtual reality mirror those observed in a real environment, particularly for depth overreach [11, 17] and lateral overreach [9, 64] in a task with vision. Similarly, lateral overreach for a proprioceptive task corroborates the results obtained in a real-world environment[55, 64].

7.2 Unimodal Data

The Figure 7 illustrates the unimodal precision and accuracy for the classical analysis method. The Figure 8 does the same for the Bayesian Analysis. Regardless the method of analysis, we observe less precision in the depth direction for the visual modality, and in the azimuthal direction for the proprioceptive modalities. Note that the depth and azimuthal directions depend on the modality, the reference point being the middle of the eyes projected on the plane of interest for the visual modality and the positions of the shoulders projected on the plane of interest for the proprioceptive modalities (left and right). With this convention, the shapes of the ellipses are relatively stable whatever the target, especially for the right proprioceptive modality.

Regardless the method, the areas of the ellipses are close when moving from one modality to the other, this result is different from the literature [64], where the visual modality has a better precision than the proprioceptive modality at least in terms of the area of the confidence ellipses. This result is discussed in section 8. We observe that one of the

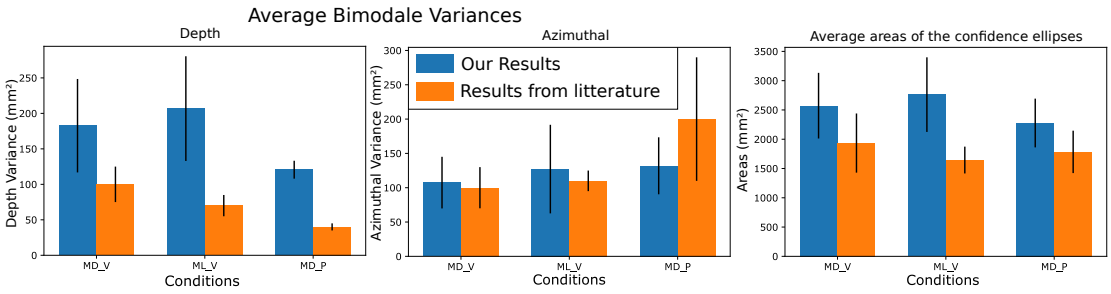

Fig. 6. Comparison of the distribution (PFI) with the literature. left and center : display of the average variances over the participants and all the targets for each condition (azimuthal variances on the left and depth variances on the right). right : display of the average areas of the confidence ellipses

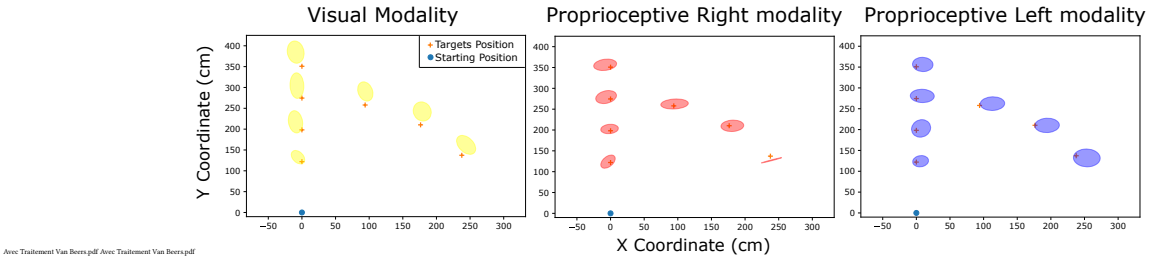

Fig. 7. Classical Analysis [64] summed up on all participants

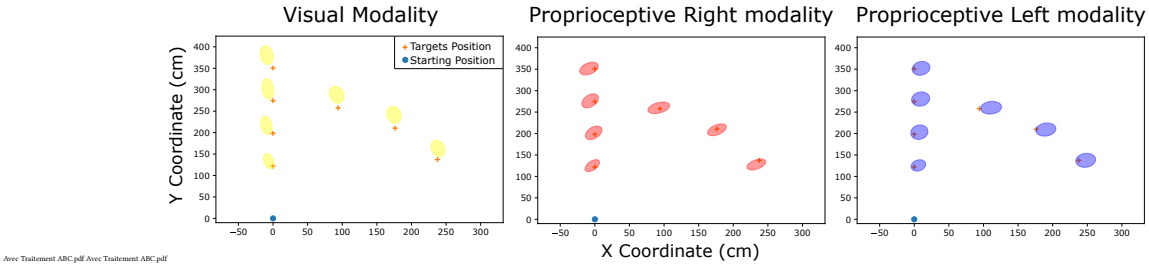

Fig. 8. ABC treatment summed on all participants

ellipses of the right proprioceptive modality is atrophied (see the rightmost ellipse of the central graph of the Figure 7). This is due to the analysis method involving subtraction and resulting in negative or almost zero variances (see section 6.2.1). This impossible result is due to the imprecision of the measurement of bimodal distributions. The Bayesian Analysis avoids these negative variances. The unimodal distributions obtained with the Bayesian Analysis have smaller areas than with the classical method. The shapes and direction of the ellipses are similar in both cases.

7.2.1 Detailed Study of the Precision Parameters. The averaged azimuthal and depth variances and covariances by modality are shown in Figure 9. We can see that the azimuthal variance is more than 2 times larger on average for right proprioception and almost 2 times larger for left proprioception than the depth variance. On the other hand, the visual variance is a little lower in the azimuthal direction than in the depth direction. Above all, we obtain azimuthal and depth variances for the visual modality that are much larger than the results of Van Beers et al. These observations are verified for both methods of analysis.

7.3 Individual Level

At the moment, we have only considered the averaged results across all participants, which has notably enabled us to compare them to previous studies that also presented results at the population level. Here we consider the results at the individual level. We have illustrated on the Figure 10 the mean of the confidence ellipses for each participant for the 3 modalities, and for the two analysis methods. For each participant it is reassuring to find a similar behavior for the two treatment methods. For example, if a participant has larger areas than his neighbors in the classical treatment, it is the same for the Bayesian Analysis. But the areas in the classical treatment are not a simple proportional increase of the areas in the Bayesian Analysis. Indeed, we do not observe the same ratios between the 3 modalities for the same

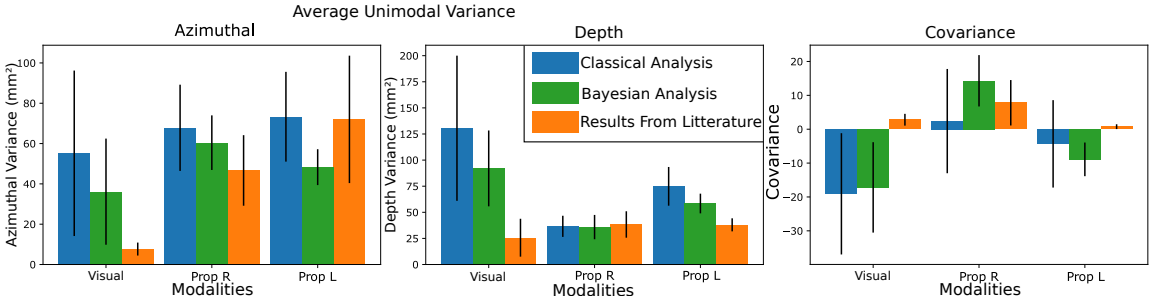

Fig. 9. Comparison of the unimodal distributions of the two analysis methods and the literature. left and center : display of the average variances over the participants and all the targets for each modalities (azimuthal variances on the left and depth variances on the right). right : display of the average covariance over the participants and all the targets for each modalities

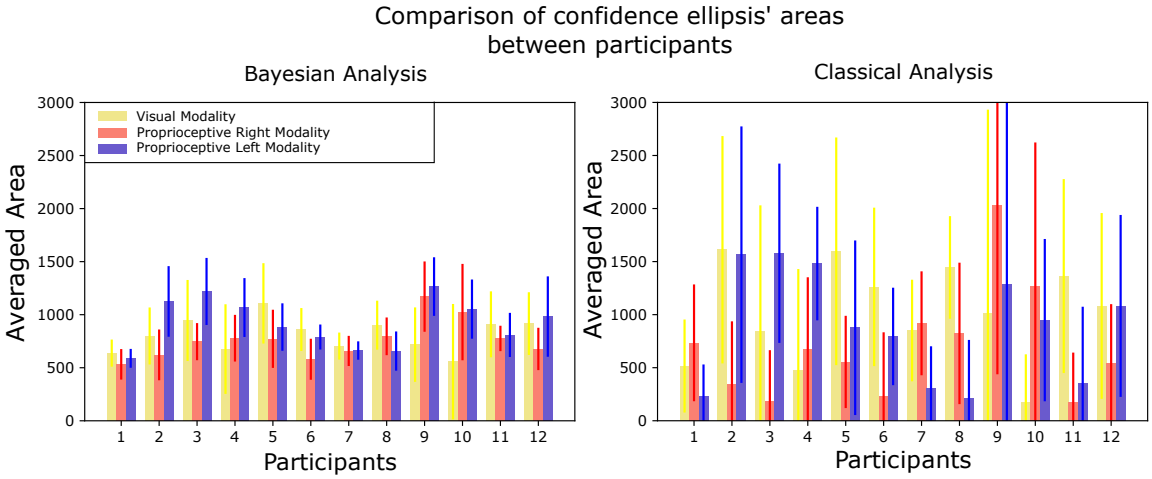

Fig. 10. Comparison of areas of mean confidence ellipses between participants for each modality.

participant for both methods.For example, participant 2 has more precision with proprioception than with vision in Bayesian analysis, but it's the opposite with classical analysis. Moreover we observe that the inter- and intra-participant variations are more marked for the classical method with a significant standard deviation for most of the participants. Even with less pronounced inter- and intra-participant differences with the Bayesian analysis, it is still possible to observe interesting patterns in certain participants. For example participant 7 has balanced precision across the three modalities. In contrast, participant 9 has a visual precision almost twice as low as his/her proprioceptive precisions. These result are discussed in section 8. Note that to streamline the article, the analysis of the evolution of precision with distance and orientation was placed in appendix B.

8 DISCUSSION

Our short-term goal was to assess the visual and proprioceptive sensory sensitivities of our participants, focusing on three research questions:

RQ1: Is there an appropriate methodology to measure visual and proprioceptive sensitivities? The protocol proposed by Van Beers [64] enables the extraction and differentiation of visual and proprioceptive sensitivities in hand movements. However, this methodology does entail certain limitations, such as the time required for conducting the data collection task, the great number of trials needed to obtain a representative distribution, and the increased complexity in data processing. Particularly, we showed that the traditional data processing method involving subtractions could yield impossible values due to the random nature of the targeting task. Instead, we decided to use a Bayesian analysis method (ABC). We demonstrated that it avoids outliers, such as negative variances or atrophied precisions. Moreover, it reduces uncertainty in our data, allowing for a better interpretation of trends.

RQ2: How are the sensory sensitivities of participants in Virtual Reality compared to those in the real world? Our results exhibit several consistencies with the existing literature. Similar to [11, 17], our participants tended to overshoot the targets in depth, and similar to [9, 64], they tended to overshoot laterally. Moreover, proprioception was more precise with respect to depth, and vision is more precise with respect to the azimuthal direction [56, 64]. However, contrary to the literature in the real world, in VR, the visual and proprioceptive accuracy measured are of the same order of magnitude. We see several possible explanations. One is that in condition $R_H - P$, the tactile information coming from the deformation of the experimental table could have helped participants to increase their precision. Another is that participants in condition $R_H - P$ remember the position of the visual target. The addition of lures after the disappearance of the visual target may not be sufficient to forget the position of this target. In this case, the distribution (PFI) in the $R_H - P$ condition would be smaller than it should be, favoring the proprioceptive sensitivities against the visual sensitivity. Finally, visual sensitivities depend on the quality of visual feedback. Despite the good quality of current visual VR interfaces (HMD), the resulting VR vision is not yet similar to real-world vision. These poor visual feedback can thus explain the "bad" visual sensitivities in VR.

RQ3: How to differentiate users based on their sensory sensitivities? We observed significant differences among participants for both analysis methods. We also observed that for Bayesian Analysis, the differences between participants are smaller. The small differences observed are certainly a consequence of the priors used in the analysis. The same priors are assigned to each participant, and the final values can be seen as a correction of the prior based on the experiment data. Therefore, it is not surprising to observe values that are relatively close and centered around the prior values for Bayesian analysis, and this can be seen as a limitation. However, we also observed a small standard deviation for most of the participants and the modalities for this analysis compared to classical analysis. Thus, any differences between participants become more significant and exploitable. In conclusion, Bayesian analysis appears to be more readily applicable for distinguishing participants based on their visual and proprioceptive sensory sensitivities. Classical analysis, while more direct, would require a larger number of trials to prevent inconsistencies in the final values.

In addressing these three research questions, we made a first step toward our long-term goal to develop adaptive visuo-haptic illusion techniques. Recently, Lebrun et al. [37] demonstrated the feasibility of adapting redirection amplitudes to each participant to increase the probability of not detecting the illusion. Their method requires a calibration task before appropriately adjusting the illusion. On the contrary, we aim to predict the optimal illusion amplitude thanks to users' sensory sensitivities. They could serve as input for a future sensorimotor model predicting the trajectories of users' hands and enabling the utilization of the comparator model [18]. We plan to use the stochastic optimal feedback control model [60] (SOFC). The interesting aspect of SOFC is the consideration of noises in motor commands and sensory perceptions. To implement the model, it is necessary to set a value for sensory noise. Usually, a significantly larger noise is assigned to proprioception compared to vision. The originality of our work is to be able to set relevant proprioceptive and visual noises for each participant. In particular, we would have more balanced visual and proprioceptive noises.

Additionally, it may be worthwhile to consider the causal inference model [36] and predict how far a virtual hand (or other limbs) can be offset from her real counterpart without disturbing the user. A user with good visual accuracy compared to his/her proprioceptive accuracy would be, for example, less likely based on the causal inference model to distinguish the virtual hand from the real hand.

9 CONCLUSION

In this paper, we motivate the relevance of studying users' visual and proprioceptive sensitivities to study the detection of visio-haptic illusions. We aim at using these sensitivities as input for computationnal model predicting the consequences of illusion implementation. We had two contributions. Our first contribution is methodological. We adapted an experimental protocol from cognitive psychology to human-computer interaction (HCI) to capture the precision of each modality from multimodal tasks, and we used a Bayesian analysis method, Approximate Bayesian Computation (ABC), not employed in the study we are drawing inspiration from for our empirical data. Our second contribution is empirical. We collected and analyzed data from 12 participants to gain a better understanding of their behavior in virtual reality.

10 AKNOWLEDGEMENT

We thank all study participants for their time, and colleagues and reviewers of IHM'24 for their helpful comments. This work is partly funded by the ANR NeuroHCI ANR22-CE33-0006-01 and the ANR Show-me ANR-20-CE33-0010.

REFERENCES

[1] Parastoo Abtahi and Sean Follmer. 2018. Visuo-haptic illusions for improving the perceived performance of shape displays. In *Proceedings of the 2018 CHI Conference on Human Factors in Computing Systems*. 1–13.

[2] Merwan Achibet, Maud Marchal, Ferran Argelaguet, and Anatole Lécuyer. 2014. The Virtual Mitten: A novel interaction paradigm for visuo-haptic manipulation of objects using grip force. In *2014 IEEE Symposium on 3D User Interfaces (3DUI)*. IEEE, 59–66.

[3] Mahdi Azmandian, Mark Hancock, Hrvoje Benko, Eyal Ofek, and Andrew D Wilson. 2016. Haptic retargeting: Dynamic repurposing of passive haptics for enhanced virtual reality experiences. In *Proceedings of the 2016 chi conference on human factors in computing systems*. 1968–1979.

[4] Yuki Ban, Takuji Narumi, Tomohiro Tanikawa, and Michitaka Hirose. 2014. Controlling perceived stiffness of pinched objects using visual feedback of hand deformation. In *2014 IEEE Haptics Symposium (HAPTICS)*. IEEE, 557–562.

[5] Peter W Battaglia, Robert A Jacobs, and Richard N Aslin. 2003. Bayesian integration of visual and auditory signals for spatial localization. *Josa a* 20, 7 (2003), 1391–1397.

[6] Hannah J Block and Brandon M Sexton. 2020. Visuo-proprioceptive control of the hand in older adults. *bioRxiv* (2020).

[7] Eric Burns, Sharif Razzaque, Abigail T Panter, Mary C Whitton, Matthew R McCallus, and Frederick P Brooks Jr. 2006. The hand is more easily fooled than the eye: Users are more sensitive to visual interpenetration than to visual-proprioceptive discrepancy. *Presence: teleoperators & virtual environments* 15, 1 (2006), 1–15.

[8] Lung-Pan Cheng, Eyal Ofek, Christian Holz, Hrvoje Benko, and Andrew D Wilson. 2017. Sparse haptic proxy: Touch feedback in virtual environments using a general passive prop. In *Proceedings of the 2017 CHI Conference on Human Factors in Computing Systems*. 3718–3728.

[9] Alan Crowe, Wim Keessen, Wim Kuus, Ronald Van Vliet, and Andre Zegeling. 1987. Proprioceptive accuracy in two dimensions. *Perceptual and motor skills* 64, 3 (1987), 831–846.

[10] Nicole David, Albert Newen, and Kai Vogeley. 2008. The "sense of agency" and its underlying cognitive and neural mechanisms. *Consciousness and cognition* 17, 2 (2008), 523–534.

[11] JB de Graaf, JFM van den Broek, H Bekkering, and AC Sittig. 1995. The visual estimation of the felt hand position is shifted towards the body midline. *Vision et adaptation* (1995), 183–192.

[12] Nandini Deshpande, Denise M Connelly, Elsie G Culham, and Patrick A Costigan. 2003. Reliability and validity of ankle proprioceptive measures. *Archives of physical medicine and rehabilitation* 84, 6 (2003), 883–889.

[13] L. Dominjon, A. Lecuyer, J. . Burkhardt, P. Richard, and S. Richir. 2005. Influence of control/display ratio on the perception of mass of manipulated objects in virtual environments. In *IEEE Proceedings. VR 2005. Virtual Reality, 2005.* 19–25. https://doi.org/10.1109/VR.2005.1492749

[14] Marc O Ernst and Martin S Banks. 2002. Humans integrate visual and haptic information in a statistically optimal fashion. *Nature* 415, 6870 (2002), 429–433.

[15] Marc O Ernst and Heinrich H Bülthoff. 2004. Merging the senses into a robust percept. *Trends in cognitive sciences* 8, 4 (2004), 162–169.

[16] Christopher R Fetsch, Gregory C DeAngelis, and Dora E Angelaki. 2010. Visual–vestibular cue integration for heading perception: applications of optimal cue integration theory. *European Journal of Neuroscience* 31, 10 (2010), 1721–1729.

[17] John M Foley and Richard Held. 1972. Visually directed pointing as a function of target distance, direction, and available cues. *Perception & Psychophysics* 12, 3 (1972), 263–268.

[18] Christopher D Frith. 1987. The positive and negative symptoms of schizophrenia reflect impairments in the perception and initiation of action. *Psychological medicine* 17, 3 (1987), 631–648.

[19] Christopher D Frith, Sarah-Jayne Blakemore, and Daniel M Wolpert. 2000. Abnormalities in the awareness and control of action. *Philosophical Transactions of the Royal Society of London. Series B: Biological Sciences* 355, 1404 (2000), 1771–1788.

[20] Shaun Gallagher. 2000. Philosophical conceptions of the self: implications for cognitive science. *Trends in cognitive sciences* 4, 1 (2000), 14–21.

[21] Benoît Geslain, Gilles Bailly, Sinan D Haliyo, and Corentin Duboc. 2021. Visuo-haptic Illusions for Motor Skill Acquisition in Virtual Reality. In *Symposium on Spatial User Interaction*. 1–9.

[22] Eric J Gonzalez, Parastoo Abtahi, and Sean Follmer. 2020. Reach+ extending the reachability of encountered-type haptics devices through dynamic redirection in vr. In *Proceedings of the 33rd Annual ACM Symposium on User Interface Software and Technology*. 236–248.

[23] Eric J Gonzalez and Sean Follmer. 2019. Investigating the detection of bimanual haptic retargeting in virtual reality. In *25th ACM Symposium on Virtual Reality Software and Technology*. 1–5.

[24] Colin Groth, Timon Scholz, Susana Castillo, Jan-Philipp Tauscher, and Marcus Magnor. 2023. Instant Hand Redirection in Virtual Reality Through Electrical Muscle Stimulation-Triggered Eye Blinks. In *Proceedings of the 29th ACM Symposium on Virtual Reality Software and Technology*. 1–11.

[25] Thor Grünbaum and Mark Schram Christensen. 2020. Measures of agency. *Neuroscience of consciousness* 2020, 1 (2020), niaa019.

[26] Hannah B Helbig and Marc O Ernst. 2007. Optimal integration of shape information from vision and touch. *Experimental brain research* 179, 4 (2007), 595–606.

[27] Denise YP Henriques, Filipp Filippopulos, Andreas Straube, and Thomas Eggert. 2014. The cerebellum is not necessary for visually driven recalibration of hand proprioception. *Neuropsychologia* 64 (2014), 195–204.

[28] D. A. G. Jauregui, F. Argelaguet, A. Olivier, M. Marchal, F. Multon, and A. Lecuyer. 2014. Toward "Pseudo-Haptic Avatars": Modifying the Visual Animation of Self-Avatar Can Simulate the Perception of Weight Lifting. *IEEE Transactions on Visualization and Computer Graphics* 20, 4 (April 2014), 654–661. https://doi.org/10.1109/TVCG.2014.45

[29] Antti Kangasrääsiö, Kumaripaba Athukorala, Andrew Howes, Jukka Corander, Samuel Kaski, and Antti Oulasvirta. 2017. Inferring cognitive models from data using approximate Bayesian computation. In *Proceedings of the 2017 CHI conference on human factors in computing systems*. 1295–1306.

[30] Shunichi Kasahara, Keina Konno, Richi Owaki, Tsubasa Nishi, Akiko Takeshita, Takayuki Ito, Shoko Kasuga, and Junichi Ushiba. 2017. Malleable embodiment: changing sense of embodiment by spatial-temporal deformation of virtual human body. In *Proceedings of the 2017 CHI Conference on Human Factors in Computing Systems*. 6438–6448.

[31] Konstantina Kilteni, Raphaela Groten, and Mel Slater. 2012. The sense of embodiment in virtual reality. *Presence: Teleoperators and Virtual Environments* 21, 4 (2012), 373–387.

[32] Konstantina Kilteni, Antonella Maselli, Konrad P Kording, and Mel Slater. 2015. Over my fake body: body ownership illusions for studying the multisensory basis of own-body perception. *Frontiers in human neuroscience* 9 (2015), 141.

[33] Luv Kohli. 2010. Redirected touching: Warping space to remap passive haptics. In *2010 IEEE Symposium on 3D User Interfaces (3DUI)*. IEEE, 129–130.

[34] Luv Kohli. 2013. Warping virtual space for low-cost haptic feedback. In *Proceedings of the ACM SIGGRAPH Symposium on Interactive 3D Graphics and Games*. 195–195.

[35] Luv Kohli, Mary C Whitton, and Frederick P Brooks. 2012. Redirected touching: The effect of warping space on task performance. In *2012 IEEE Symposium on 3D User Interfaces (3DUI)*. IEEE, 105–112.

[36] Konrad P Körding, Ulrik Beierholm, Wei Ji Ma, Steven Quartz, Joshua B Tenenbaum, and Ladan Shams. 2007. Causal inference in multisensory perception. *PLoS one* 2, 9 (2007), e943.

[37] Flavien Lebrun, Sinan Haliyo, and Gilles Bailly. 2021. A Trajectory Model for Desktop-Scale Hand Redirection in Virtual Reality. In *IFIP Conference on Human-Computer Interaction*. Springer, 105–124.

[38] Anatole Lécuyer. 2009. Simulating haptic feedback using vision: A survey of research and applications of pseudo-haptic feedback. *Presence: Teleoperators and Virtual Environments* 18, 1 (2009), 39–53.

[39] Anatole Lécuyer, J-M Burkhardt, Sabine Coquillart, and Philippe Coiffet. 2001. " Boundary of illusion": an experiment of sensory integration with a pseudo-haptic system. In *Proceedings IEEE Virtual Reality 2001*. IEEE, 115–122.

[40] Jarno Lintusaari, Henri Vuollekoski, Antti Kangasrääsiö, Kusti Skytén, Marko Järvenpää, Pekka Marttinen, Michael U. Gutmann, Aki Vehtari, Jukka Corander, and Samuel Kaski. 2018. ELFI: Engine for Likelihood-Free Inference. *Journal of Machine Learning Research* 19, 16 (2018), 1–7. http://jmlr.org/papers/v19/17-374.html

[41] Paul R MacNeilage, Martin S Banks, Daniel R Berger, and Heinrich H Bülthoff. 2007. A Bayesian model of the disambiguation of gravitoinertial force by visual cues. *Experimental Brain Research* 179, 2 (2007), 263–290.

[42] Kazumichi Matsumiya. 2019. Separate multisensory integration processes for ownership and localization of body parts. *Scientific reports* 9, 1 (2019), 1–9.

[43] R Chris Miall and Daniel M Wolpert. 1996. Forward models for physiological motor control. *Neural networks* 9, 8 (1996), 1265–1279.

[44] Nami Ogawa, Takuji Narumi, and Michitaka Hirose. 2020. Effect of avatar appearance on detection thresholds for remapped hand movements. *IEEE transactions on visualization and computer graphics* 27, 7 (2020), 3182–3197.
[45] Gonçalo Padrao, Mar Gonzalez-Franco, Maria V Sanchez-Vives, Mel Slater, and Antoni Rodriguez-Fornells. 2016. Violating body movement semantics: Neural signatures of self-generated and external-generated errors. *Neuroimage* 124 (2016), 147–156.
[46] Francesco Pavani, Charles Spence, and Jon Driver. 2000. Visual capture of touch: Out-of-the-body experiences with rubber gloves. *Psychological science* 11, 5 (2000), 353–359.
[47] Parinya Punpongsanon, Daisuke Iwai, and Kosuke Sato. 2015. Softar: Visually manipulating haptic softness perception in spatial augmented reality. *IEEE transactions on visualization and computer graphics* 21, 11 (2015), 1279–1288.
[48] Sharif Razzaque. 2005. *Redirected walking*. The University of North Carolina at Chapel Hill.
[49] Johanna Reuschel, Knut Drewing, Denise YP Henriques, Frank Rösler, and Katja Fiehler. 2010. Optimal integration of visual and proprioceptive movement information for the perception of trajectory geometry. *Experimental brain research* 201, 4 (2010), 853–862.
[50] Bernhard E Riecke, Aleksander Väljamäe, and Jörg Schulte-Pelkum. 2009. Moving sounds enhance the visually-induced self-motion illusion (circular vection) in virtual reality. *ACM Transactions on Applied Perception (TAP)* 6, 2 (2009), 1–27.
[51] Michael Rietzler, Florian Geiselhart, Jan Gugenheimer, and Enrico Rukzio. 2018. Breaking the tracking: Enabling weight perception using perceivable tracking offsets. In *Proceedings of the 2018 CHI Conference on Human Factors in Computing Systems*. 1–12.
[52] Majed Samad, Albert Jin Chung, and Ladan Shams. 2015. Perception of body ownership is driven by Bayesian sensory inference. *PloS one* 10, 2 (2015), e0117178.
[53] Majed Samad, Elia Gatti, Anne Hermes, Hrvoje Benko, and Cesare Parise. 2019. Pseudo-haptic weight: Changing the perceived weight of virtual objects by manipulating control-display ratio. In *Proceedings of the 2019 CHI Conference on Human Factors in Computing Systems*. 1–13.
[54] Moritz Schubert and Dominik Endres. 2021. The Bayesian Causal Inference of Body Ownership Model: Use in VR and Plausible Parameter Choices. In *2021 IEEE Conference on Virtual Reality and 3D User Interfaces Abstracts and Workshops (VRW)*. IEEE, 67–70.
[55] R Townley Slinger and Victor Horsley. 1906. Upon the orientation of points in space by the muscular, arthrodial, and tactile senses of the upper limbs in normal individuals and in blind persons. *Brain* 29, 1 (1906), 1–27.
[56] Hendrikus J Snijders, Nicholas P Holmes, and Charles Spence. 2007. Direction-dependent integration of vision and proprioception in reaching under the influence of the mirror illusion. *Neuropsychologia* 45, 3 (2007), 496–505.
[57] Samuel J Sober and Philip N Sabes. 2003. Multisensory integration during motor planning. *Journal of Neuroscience* 23, 18 (2003), 6982–6992.
[58] Samuel J Sober and Philip N Sabes. 2005. Flexible strategies for sensory integration during motor planning. *Nature neuroscience* 8, 4 (2005), 490–497.
[59] Robert L Solso, M Kimberly MacLin, and Otto H MacLin. 2005. *Cognitive psychology*. Pearson Education New Zealand.
[60] Emanuel Todorov. 2005. Stochastic optimal control and estimation methods adapted to the noise characteristics of the sensorimotor system. *Neural computation* 17, 5 (2005), 1084–1108.
[61] Manos Tsakiris, Gita Prabhu, and Patrick Haggard. 2006. Having a body versus moving your body: How agency structures body-ownership. *Consciousness and cognition* 15, 2 (2006), 423–432.
[62] William WN Tsang and Christina WY Hui-Chan. 2003. Effects of tai chi on joint proprioception and stability limits in elderly subjects. *Medicine & Science in Sports & Exercise* (2003).
[63] Yusuke Ujitoko and Yuki Ban. 2021. Survey of pseudo-haptics: Haptic feedback design and application proposals. *IEEE Transactions on Haptics* 14, 4 (2021), 699–711.
[64] Robert J Van Beers, Anne C Sittig, and Jan J Denier van der Gon. 1998. The precision of proprioceptive position sense. *Experimental brain research* 122, 4 (1998), 367–377.
[65] Robert J Van Beers, Anne C Sittig, and Jan J Denier van der Gon. 1999. Integration of proprioceptive and visual position-information: An experimentally supported model. *Journal of neurophysiology* 81, 3 (1999), 1355–1364.
[66] Robert J van Beers, Daniel M Wolpert, and Patrick Haggard. 2002. When feeling is more important than seeing in sensorimotor adaptation. *Current biology* 12, 10 (2002), 834–837.
[67] Loes CJ van Dam and Marc O Ernst. 2013. Knowing each random error of our ways, but hardly correcting for it: An instance of optimal performance. *PloS one* 8, 10 (2013).
[68] Daniel M Wolpert and Zoubin Ghahramani. 2000. Computational principles of movement neuroscience. *Nature neuroscience* 3, 11 (2000), 1212–1217.
[69] André Zenner and Antonio Krüger. 2019. Estimating detection thresholds for desktop-scale hand redirection in virtual reality. In *2019 IEEE Conference on Virtual Reality and 3D User Interfaces (VR)*. IEEE, 47–55.
[70] Lionel H Zupan, Daniel M Merfeld, and Christian Darlot. 2002. Using sensory weighting to model the influence of canal, otolith and visual cues on spatial orientation and eye movements. *Biological cybernetics* 86, 3 (2002), 209–230.

A THE COMPARATOR MODEL

The mechanism that is frequently cited as the best explanation of SoA is the so-called **comparator model** (see Figure 11). According to this model, the SoA occurs when the prediction of the sensory consequence of an action matches the actual sensory feedback at the end of the action. When the brain creates a motor signal, it also generates a copy of this

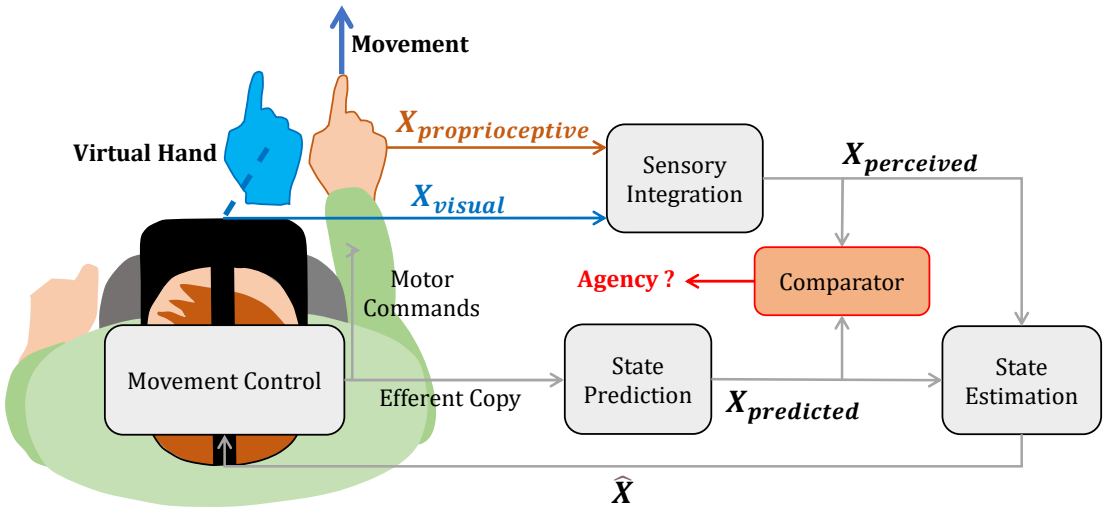

Fig. 11. Diagram of the comparator model [18]. An efferent copy is emitted with the emission of a motor command. A prediction of the sensory consequence of an action calculated based on the efferent copy is compared to the actual sensory feedback. If the two information are significantly close, a strong sense of Agency is experienced. In our case, the visual sensory information is perturbed by the implementation of the illusion.

motor command called "efferent copy". The sensory perception is then predicted based on this efferent copy [43, 68]. When the predicted and actual perceptions match, a strong SoA is experienced [19]. The comparator model can explain why we experience Agency over a virtual avatar. The pertinence of the comparator model is reinforced by the fact that the user representation does not have to be realistic. Even if the arm of the user is represented by a sphere in VR, the SoA over the sphere is possible if it mimics arm movement.

B EVOLUTION OF PRECISION WITH DISTANCE AND ORIENTATION

Interpreting the evolution of unimodal precision as a function of target position is difficult by looking only at the confidence ellipses in figures Figure 7 and Figure 8. We therefore display on Figure 12 the evolution of the mean of the areas of the confidence ellipses (and their standard deviation) as a function of the distance to the reference point of each modality (the depth r) for the two analysis methods. We note that for both analysis methods and for all modalities the areas increase with depth. Even if the classical treatment method presents important area variations, the large standard deviations prevent a clear reading of the results. This is why in the rest of this section we only present the curves obtained with the Bayesian Analysis.

On the Figure 13 we observe the azimuthal and depth variances as a function of r for the Bayesian analysis. We explain by these graphs the evolution of the areas of the Figure 12. We notice that the azimuthal variances of the proprioceptive modalities are increasing with r in contrast to their more stable depth variances. On the contrary, the visual modality is more stable in azimuth and varies strongly in depth. Thus it seems that the precision are stable in their most precise direction (depth for vision and azimuth for proprioception).

We study on the Figure 14 the evolution of the variances and the area of the confidence ellipses as a function of the orientation θ of the target with respect to the reference axis of each modality (perpendicular to the thorax and centered: at the middle of the body for vision, 200mm to the right or to the left for the respective proprioceptions). The azimuthal

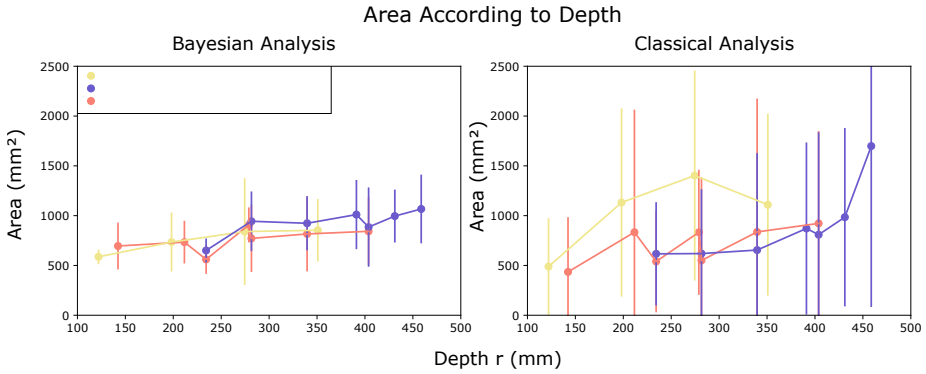

Fig. 12. Evolution of areas according to distance for the two methods of analysis for the 3 modalities

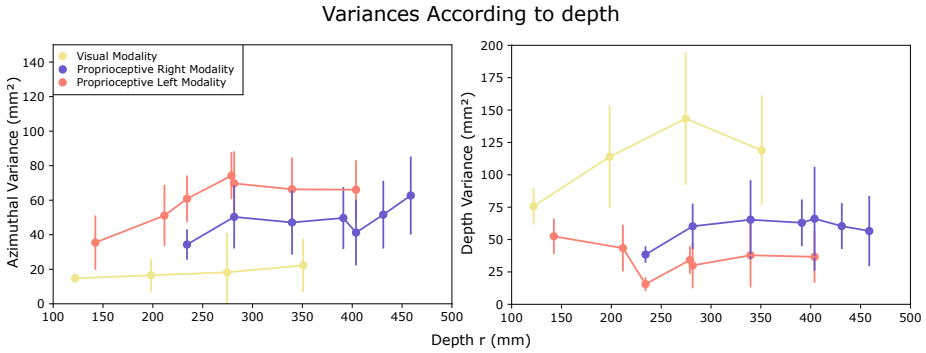

Fig. 13. Evolution of azimuthal and depth variances for the 3 modalities according to depth r for the Bayesian analysis.

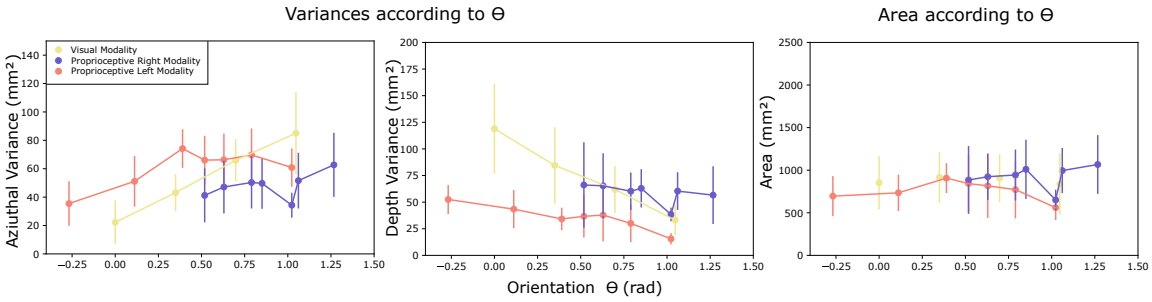

Fig. 14. Evolution of areas and variances according to orientation for the 3 modalities for the Bayesian Analysis

variances are increasing with θ and the depth variances are decreasing. This explains the relative stability of the area with respect to θ. Note that it is the visual modality that seems to be the most sensitive to θ.

Exploiting these evolutions can help create from little data the precision of a modality and a prediction of how it will be impacted by a shift in space.